Geometrical shape dependence field emission from patterned carbon nanotube array: A simulation based study

Rajkumar Patra[*], **Himani Sharma, Swati Singh, S. Ghosh, V. D. Vankar**

*Nanostech Laboratory, Department of Physics, Indian Institute of Technology Delhi, New Delhi 16, India*

[*]Corresponding author. Tel: (+91) 11-26591329; Fax: (+91) 11-26581114; E-mail: rajkumar.patra@physics.iitd.ac.in

ABSTRACT

Designing an efficient field emission source requires theoretical optimization of electron emitters' geometrical distribution over the surface for its best performance in terms of current density. Seven and nineteen bundles of CNT arrays arranged in different models are analysed in detail using a computational theory in CST studio suite software based on the particle tracking mode. A three dimensional model has been employed to calculate FE properties with high accuracy. Simulations were carried out for a particular number of CNTs of constant height and radius located at fixed distances from each other and arranged in different geometrical patterns. Among all patterns, rectangular arrangement of CNTs is found to produce the maximum current. The edge effect and screening effect are incorporated in calculating total emission current and are found to diminish the contribution of inner rings 10% or less than that of maximum contribution. These findings can be employed as guideline to fabricate pattered CNT structures experimentally for industry applications. Copyright © 2014 VBRI press.

Keywords: Field emission; simulation; carbon nanotube; patterning.
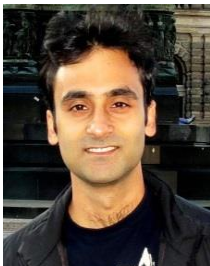
Rajkumar Patra has completed his M.Sc. in Physics from Indian Institute of Technology Roorkee in 2008. Currently, he is pursuing his Ph.D. as senior research fellow from Department of Physics, Indian Institute of Technology Delhi, India. His area of interest is field emission, carbon nanotube and carbon nanotube based composites.

Himani Sharma received her Ph. D degree in Physics (2012) from Indian Institute of Technology Delhi, India. Presently, she is working as a postdoctoral fellow in University of Alberta. Her research work is focused on the carbon dioxide photoreduction.

Vasant D. Vankar is currently a Professor Emeritus in the Department of Physics, Indian Institute of Technology Delhi, India. He obtained his Ph.D. in Physics from Banaras Hindu University, Varanasi, India. His research interests are in Nanotechnology, Carbon Nanotubes and Graphene thin films, plasma processing of materials, solid state interfaces, phase change materials for optical recording, hard coating, macro-crystalline diamond, diamond like Carbon and surface physics. In

these areas of research, he has published about more than 130 research papers in International Journals and One US Patent on Boron Nitride and related coatings.

Introduction

Field electron emission sources are essential elements in a variety of applications that includes electron microscopes, cathode-ray tube monitors, microwave amplifiers *etc* [1]. Field emitters have attracted more attention than other electron sources due to their low turn-on and threshold fields, functionality at room temperature, ultrahigh brightness, tunable emission area and miniaturized device size.[2-6] Carbon nanotubes (CNTs) with their intriguing structure, nanometer scale sharp tips and high aspect ratio, are most promising materials to be used for field emission display devices, vacuum electronic devices, microscopy techniques, lithography systems and industrial electron-beam applications [7-9].

Low work function, low turn on and threshold fields and high field enhancement factor *(β)* are essential parameter to enhance FE characteristics of emitters. Other parameters like separation between emission sites, length of emitter and the structure at the emitter tip influence *β* and hence the FE efficiency of an emitter. Along with geometrical structure and aspect ratio, one of the most important parameter that affects FE is controlled number density of

emitters. Highly dense growth of CNTs leads to screening effect by neighboring CNTs [10, 11]. It is reported that the screening effect is reduced when the separation between CNTs is twice of their height [12-14]. So, in order to get enhanced electron emission, the screening effect is to be minimized which requires a controlled and patterned growth of CNTs. Many groups have reported both simulation and experiment based studies from patterned CNTs arrays/pillars to achieve better FE properties [11, 15-17] due to edge effect. Kilian *et al.* have reported excellent FE properties (low turn on field 0.9 V/μm and stable current densities as high as 10 mA/cm^2 at an applied macroscopic field of 5.7 V/μm) from CNT pillars due to edge effect which leads to the enhancement of electric field along the edge of each pillar [18]. However, isolated CNTs with uncontrolled distribution are not a reliable design from device applications point of view. The reliable cathode design must guarantee a stable operation at a high current [19]. So, controlled distribution of CNTs with different designs should provide high current values and enhanced field emission. To develop a design/architecture from device fabrication point of view using CNT emitters is a challenging task.

The main objective of this work is to simulate CNTs placed in different geometrical shape to find out best pattern, which shows the least screened highest emission current, and to extrapolate the result to predict the number of CNTs for a device. We have carried out a detailed quantitative investigation of the FE characteristics keeping these problems in mind. This paper presents simulation of FE properties from CNT arrays arranged in various designs. We first simulated a single CNT to investigate the local electric field. Afterwards, arrays of seven and nineteen CNTs with different designs were simulated in order to investigate the local field and total current values. The various designs of CNT arrays used for simulation were circular, square, rectangular, triangular and rhomboidal. Furthermore, from the simulation results we found out the current contribution from inner rings in a system of CNT arrays of different shapes, which is fitted to predict the approximate number of CNTs, required to obtain a desired current value. The novelty of this work lies in finding out the number of the CNTs within a particular pattern for electron emission based applications considering screening effect and edge effect. This simulation predicts the numbers of emitters, number of less contributing ring in a particular pattern and emission current for a device with particular patterning without doing real experiment which is the main advantage of this work.

Simulation

Field emission current of patterned CNTs were simulated using CST studio suite software in particle tracking mode, which uses finite integration technique along with perfect boundary approximation. This numerical method provides a universal spatial discretization scheme applicable to various electromagnetic problems including static field calculations. Creating a suitable mesh system splits this domain up into many small elements, or grid cells. The spatial discretization of Maxwell's equations is finally performed on two orthogonal grid systems where the degrees of freedom are introduced as integral value. Now Maxwell's equations are formulated for each of the cell

facets. The simulated structure and the electromagnetic fields are mapped to hexagonal mesh. Particle tracking solver is used to compute trajectories of charged particles within an electrostatic field. Gun-iterations enable computation of self-consistent electric field. Surfaces defined as particle sources emit charged particles considering a predefined field induced emission model. The software calculates particle trajectories, electrostatic field, space-charge distribution and particle current. Simulations were performed over different geometries of CNT bundles to calculate the total particle current, individual particle source current, enhanced electric field at each particle source tip and potential distribution.

Results and discussion

A model of a single, close-ended, vertically aligned CNT with a height h and radius r, comprising of a long cylindrical tube mounted with a hemispherical cap placed in conventional diode geometry is shown in **Fig. 1(a)**. The CNT is placed on the cathode which is grounded and is separated by a distance d from an anode, which is at a positive potential. The suitable mesh system is created that splits up the domain grid cells. The mesh generation view in the model of single CNT is shown in **Fig. 1(b)**. It is seen that the mesh lines become narrower over the CNT tip which is the source of electrons. Here, it is assumed that emission takes place from CNT tip only and not from its sides. The field pattern of single CNT model is shown in **Fig. 1(c)**.
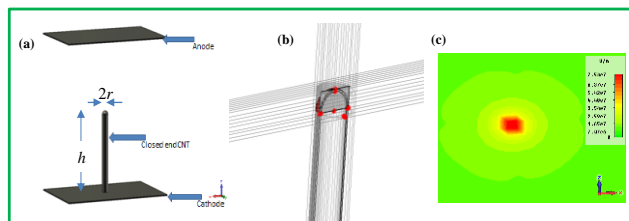

Fig. 1. Schematic model of (a) close ended single vertically aligned CNT. (b) Mesh generation view of the single CNT. (c) The field pattern of single CNT.

For sake of calculation, in this model applied voltage difference between the anode and the cathode is 200V and the distance between anode and cathode is d =20 μm. Other details of the parameters are given in **Table 1**. The local electric field value at tip of CNT is observed to be highest $(1.59 \times 10^7$ V/m) than that found at other part of the tube.

Table 1. Parameters used for the simulation of CNT arrays of different shapes.

Different models of CNT array	Total current (A)
Circular model	1.39000×10^{-7}
Triangular model	1.11410×10^{-7}
Square model	6.20549×10^{-8}
Rectangular model	1.14572×10^{-7}
Rhombus model	6.37475×10^{-8}

Simulations are performed on CNT arrays (individual CNT radius r = 5 nm and height h = 5 μm) of seven and nineteen CNTs by keeping them at the center and at the

periphery of a circle, square, rectangle, triangle and rhombus at inter-tube distance of 5 μm. These models are named as circular, square, rectangular, triangular and rhombus model. For 7 CNT array, we placed six CNTs on a ring around one placed at the center whereas for 19 CNT array, we placed eighteen CNTs on two rings apart from one placed at the center. Fowler-Nordheim (FN) potential barrier for field emission of all CNTs has been considered. The field enhancement factor ($\beta = h/r$) is taken as 1000, applied electric field is 10V/μm and work function of CNTs is 4.5 eV.

The seven CNT arrays with different configurations are shown in Fig. 2. The electric field values from the simulated CNTs are taken at the CNT tips by keeping the inter-tube separation same. The electric field distribution at the CNT tips for the circular configuration of CNTs is shown in **Fig. 2(a)**. Similarly, the electric fields for triangular, square, rectangular and rhombus models are shown in **Figs. 2(b) - 2(e)**, respectively. Basically, the color contrast in the contour plot provides the field strength distribution; the brighter the spot, the stronger the field is [**19**].
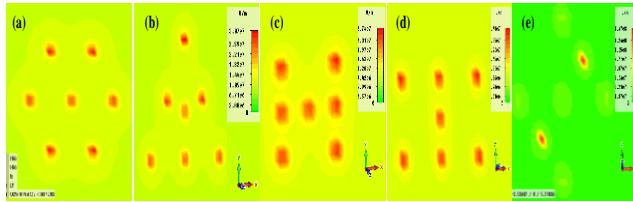

Fig. 2. The field pattern of 7 CNTs arranged in (a) Circle, (b) Triangle, (c) Square, (d) Rectangle, (e) Rhombus shape.

However, in the present case, the electric field values for the bundle of seven CNTs are found almost same with a small variation for different shapes. But, the emitted current is observed to vary at different points due to different shapes of the arrays. The field and current values are taken at all the seven points for all models. The total current emitted from the seven CNTs for various models are enlisted in **Table 2**. The best total current is observed for circular configuration (1.39×10^{-7} A) followed by rectangular configuration (1.14×10^{-7} A), triangular configuration (1.11×10^{-7} A), rhombus configuration (6.37×10^{-8} A) and square configuration (6.20×10^{-8} A). It is seen in **Fig. 2** that all the defined shapes in the seven bundled CNTs exhibit uniform field distribution except that of rhombus shape.

Table 2. Values of total current emitted from an array of seven CNTs of various models.

Various parameters used for simulation	Parameter Values used
Anode potential	200 V
Cathode potential	0.0 V
Radius of CNTs	5.0 nm
Height of CNTs	5.0 μm
Distance between cathode and anode	20 μm
Inter-tube separation	5.0 μm
Work function	4.5 eV
Length of electrodes	50 μm
Thickness of electrodes	0.5 μm

The nineteen CNTs bundle with different models is shown in **Fig. 3**. The electric field and potential distribution above the CNT tips for the circular, triangular, rectangular, square and rhombus models are shown in **Fig. 3(a) - 3(j)**, respectively. The similar simulations were carried for all these models with increased number of CNTs keeping other parameters constant. The variation in the color contrast of CNT emitters is seen in **Fig. 3**.
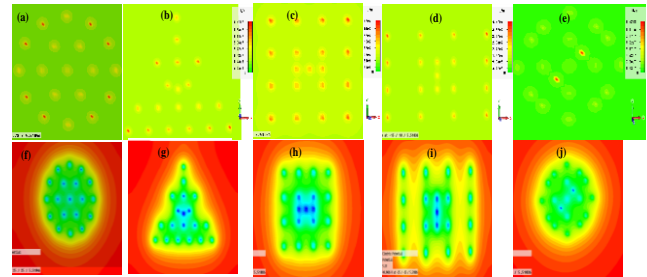

Fig. 3. The field pattern of 19 CNTs arranged in (a) circle, (b) Triangle, (c) Square, (d) Rectangle, (e) Rhombus shape and potential distribution of 19 CNTs arranged in (f) Circle, (g) Triangle, (h) Square, (i) Rectangle, (j) Rhombus shape.

The corner emitters are brighter in comparison to the center emitters which can be explained by screening effect. The CNTs at the center exhibit almost similar field values at the center. However, at the edges, the field values change and are higher in comparison to the center. It means that the CNTs at the center get screened in comparison to the edges. The local field values vary in array of nineteen CNTs in comparison to that of seven CNTs. Out of various defined shapes used for simulation, the CNTs in a square array exhibit uniform field. For all other shapes, the field varies from center to the edges. The different order of total current is also achieved. The maximum total current (**Table 3**) is achieved for rectangular model (3.55×10^{-7} A) followed by triangular (2.55×10^{-7} A), circular (2.47×10^{-7} A), square (1.98×10^{-7} A) and rhombus (8.82×10^{-8} A). The total current in each model is found to increase with increased number of CNTs due to increment in emitter sites. But practically, due to screening effect, edge effect, space charge effect the increment in emission current for a particular number of CNTs is less than that predicted theoretically which in turn reduces the local electric field and hence the enhancement factor.

Table 3. Values of total current emitted from an array of 19 CNTs of various models.

Different models of CNT arrays	Total current (A)
Circular model	2.47000×10^{-7}
Triangular model	2.54641×10^{-7}
Square model	1.98190×10^{-7}
Rectangular model	3.55540×10^{-7}
Rhombus model	8.81647×10^{-8}

In order to extrapolate the total emission current from a bundle containing large number of CNTs, we have tried to fit the simulated current from each of the rings in a bundle of 19 CNTs patterned in the rectangular geometry and extended it for larger number of rings (**Fig. 4**).
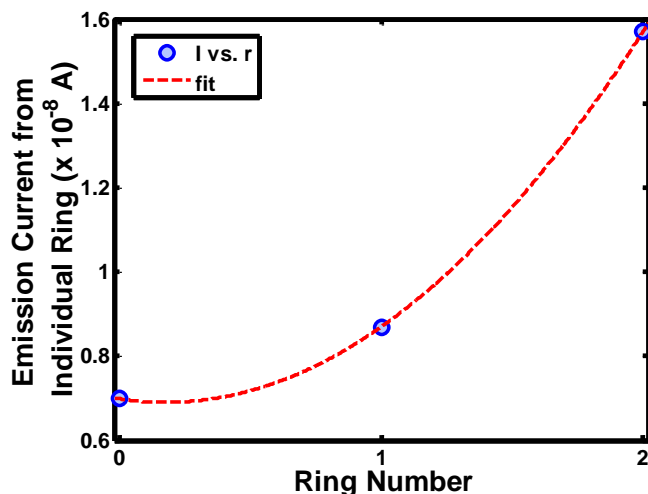
Fig. 4. Emission current from individual ring versus ring number for rectangular geometry and fitting of the simulated data.

The simulated data is fitted by the equation:

$$I = mr^2 + nr + p$$

where $m = 2.655 \times 10^{-9}$, $n = -9.55 \times 10^{-10}$ and $p = 6.99 \times 10^{-9}$ and r is the ring number. For a system of large number of rings, the current of the outer ring is found to saturate towards 10^{-3} A, shown in **Fig. 5**.
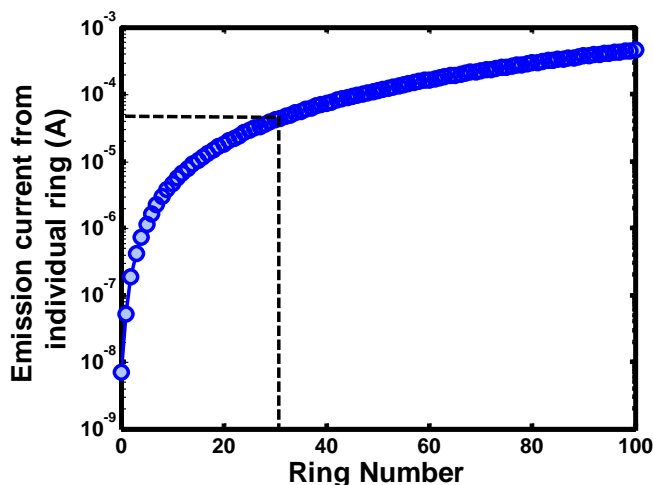

Fig. 5. Plot of emission current from individual ring calculated from fitting versus ring number to find the ignored contribution of a system of 100 rings.

This shows that the current up to 31 inner rings in circular pattern contributes less than 10% of the current from the outer ring. So, the current contribution from the inner 31 rings can be ignored with respect to outer ring. The observed decrement in the emission current could be due to screening effect. This result also shows that the emission current from the outer rings of a rectangular pattern containing array of 100 rings is saturating towards a maximum current value of 10^{-3}A. Also from this fitting, the number of rings of ignored contribution found is ~ 30% (precisely 31.62%) within a system of any shape. This study also indicates that in order to achieve a current

density of 100 μA/cm^2, array of 6769 numbers of CNTs of tube-radius 5 nm and tube-height 5 μm need to be arranged within 47 rings in rectangular pattern with inter-tube separation 5 μm.

Conclusion

A detailed simulated field emission study is performed for single CNT, an array of 7 CNTs and an array of 19 CNTs arranged in different patterns to investigate the shape dependence of emission current for patterned CNTs. Also, the contributing number of rings is found out for each shape by fitting the obtained results to study the edge effect and screening effect for ring system array in patterned CNTs. The whole study leads to the conclusion that rectangular shape is the best among all and gives maximum field emission current for patterned model of large number CNTs. Also, it is found that for a sample of large rings, 31.62% of inner rings are contributing 10% or less than that of maximum contribution of individual ring for any shape due to edge effect and screening effect. In addition to this, one can predict number of CNTs to keep in a particular geometry to achieve a desired current density without doing actual experiment. In future, this work can be used to choose the geometrical shape for patterning and to simulate out packing density of the CNT emitters in field emission devices. Also, the effective emissive area of the sample can be approximate from this work.

Reference

1. Saito, Y.; Uemura S.; *Carbon* **2000**, *38*, 169.
   DOI: 10.1016/S0008-6223(99)00139-6
2. Patra, R..; Ghosh, S.; Sharma, H.; Vankar, V.D.; *Adv. Mat. Lett.* **2013**, 4, 849.
   DOI: 10.1063/1.4874435
3. Sarker, D.; Kumar, H.; Patra, R.; Kabiraj, D.; Avasthi, D. K.; Vayalil, S. K.; Roth, S. V., Srivastava, P.; Ghosh, S.; *J. Appl. Phys.* **2014**, *115*, 174304.
   DOI: 10.1063/1.4874435
4. Patra, R.; Ghosh, S.; Sheremet, E.; Jha, M.; Rodriguez, R. D.; Lehman,
   D.; Ganguli, A. K.; Gordon, O. D.; Schmidt, H.; Schulze, S.; Zahn, D. R. T.; Schmidt, O. G.; *J. Appl. Phys.* **2014**, *115*, 094302.
   DOI: 10.1063/1.4866990
5. Jha, M.; Patra, R.; Ghosh, S.; Ganguli, A. K.; *J. Mater. Chem.* **2012**, *22*, 6356.
   DOI: 10.1039/C2JM16538D
6. Jha, M.; Patra, R.; Ghosh, S.; Ganguli, A. K.; *RSC Adv.* **2012**, *2*, 7875.
   DOI: 10.1039/C2RA20399E
7. Choi, W. B.; Chung, D. S.; Kang, J. H.; Kim, H. Y.; Jin, Y. W.; Han, I. T.; Lee, Y. H.; Jung, J. E.; Lee, N. S.; Park, G. S.; Kim, J. M; *Appl. Phys. Lett.* **1999**, *75*, 3129.
   DOI: 10.1063/1.125253
8. Saito, Y. (Ed.); Carbon Nanotube and Related Field Emitters: Fundamentals and Applications; Wiley: Germany, **2010**.
   ISBN: 9783527630615
9. De Jonge, N.; Bonard, J. M.; *Philos. T. R. Soc. A* **2004**, *362*, 2239.
   DOI: 10.1098/rsta.2004.1438
10. Chiu, C. C.; Tsai, T. U.; Tai, N. H.; *Nanotechnology.* **2006**, *17*, 2840.
    DOI: 10.1088/0957-4484/17/12/002
11. Cai, D.; Liu, L.; *AIP Adv.* **2013**, *3*, 122103.
    DOI: 10.1063/1.4841275
12. Smith, R. C.; Silva, S. R.; *Appl. Phys. Lett.* **2009**, *94*, 133104.

DOI: 10.1063/1.3097239

13. Bonard, J.M.; Salvetat, J.P.; Stockli, T.; Forra, L.; Chatelain, A.; *Appl. Phys. A: Mater. Sci. Process.***1999**, *69*, 245.
DOI: 10.1007/s003390050998

14. Nilsson, L.; Groening, O.; Emmenegger, C.; Kuettel, O.; Schaller, E.; Schlapbach, L.;Kind, H.; Bonard J. M.; Kern K.; *Appl. Phys. Lett.* **2000**, *76*, 2071.
DOI: 10.1063/1.126258

15. Tsai, C. N.; Kirkici, H.; *IEEE T. Electron. Dev.*, **2013**, *60*, 478.
DOI: 10.1109/TED.2012.2227970

16. Wang, S.; Sellin, P. J.; Lian, J.; Ozsan, E.; Chang, S.; *Curr. Nanosci.* **2009**, *5*, 54.
DOI: 10.2174/157341309787314638

17. Sohn, J. I.; Lee, S.; Song, Y. H.; Choi, S. Y.; Cho, K. I.; Nam, K. S.; *Appl. Phys. Lett.* **2001**, *78*, 901.
DOI: 10.1063/1.1335846

18. Killian, J. L.; Zuckerman, N. B.; Niemann, D. L.; Ribaya, B. P.; Rahman, M.; Espinosa, R.; Meyyappan, M.; Nguyen, C. V.; *J. Appl. Phys.* **2008**,*103,* 064312.
DOI: 10.1063/1.2870931

19. Hong, N.T.; Koh, K. H.; Lee, S.; Minh, P. N.; Tam, N. T. T.; Khoi, P. H.; *J. Vac. Sci. Technol. B* **2009**, *27*, 749.
DOI: 10.1116/1.3097850